



Open Research Online

The Open University's repository of research publications and other research outputs

Anisotropic oxygen diffusion in tetragonal $\text{La}_2\text{NiO}_{4+}$: molecular dynamics calculations

Journal Item

How to cite:

Chroneos, Alexander; Parfitt, David; Kilner, John A. and Grimes, Robin W. (2010). Anisotropic oxygen diffusion in tetragonal $\text{La}_2\text{NiO}_{4+}$: molecular dynamics calculations. *Journal of Materials Chemistry*, 20(2) pp. 266–270.

For guidance on citations see [FAQs](#).

© 2010 The Royal Society of Chemistry

Version: Version of Record

Link(s) to article on publisher's website:

<http://dx.doi.org/doi:10.1039/b917118e>

<http://pubs.rsc.org/en/Content/ArticleLanding/2010/JM/b917118e>

Copyright and Moral Rights for the articles on this site are retained by the individual authors and/or other copyright owners. For more information on Open Research Online's data [policy](#) on reuse of materials please consult the policies page.

oro.open.ac.uk

Anisotropic oxygen diffusion in tetragonal $\text{La}_2\text{NiO}_{4+\delta}$: molecular dynamics calculations

Alexander Chroneos,* David Parfitt, John A. Kilner and Robin W. Grimes

Received 19th August 2009, Accepted 1st October 2009

First published as an Advance Article on the web 30th October 2009

DOI: 10.1039/b917118e

Molecular dynamics simulations, used in conjunction with a set of Born model potentials, have been employed to study oxygen transport in tetragonal $\text{La}_2\text{NiO}_{4+\delta}$. We predict an interstitialcy mechanism with an activation energy of migration of 0.51 eV in the temperature range 800–1100 K. The simulations are consistent with the most recent experiments. The prevalence of oxygen diffusion in the a – b plane accounts for the anisotropy observed in measurements of diffusivity in tetragonal $\text{La}_2\text{NiO}_{4+\delta}$.

Introduction

A number of oxides are presently being investigated for solid-oxide fuel cell (SOFC) electrode applications. These materials must have improved performance at lower temperatures and resistance to degradation during operation. In this regard, perovskite-related materials such as the Ruddlesden-Popper (RP) series of layered oxides (formula $\text{A}_{n+1}\text{B}_n\text{O}_{3n+1}$) are important candidate materials for the next generation of SOFCs because of their electrochemical, electrical and catalytic properties in synergy with their thermal and mechanical stability. In particular, La_2NiO_4 and related materials with the K_2NiF_4 structure (A_2BO_4 or the first members of the RP series) are considered for oxygen sensors, oxygen separation membranes and as cathodes for intermediate temperature SOFCs (ITSOFCs).^{1–12} These materials exhibit an oxygen hyperstoichiometry that significantly influences the oxygen transport (see for example ref. 3 and references therein). Interestingly, previous experimental studies report a wide range of determined activation energies, from 0.19 eV to 0.90 eV and the mechanism of diffusion is not well defined.^{2,5,13} This range includes both studies of total diffusion and a – b plane and c direction partial diffusions measured for single crystals and/or thin films.

The knowledge of the crystal structure, stoichiometry and the effect of different A and B atoms are important in the study of diffusion mechanisms.^{10,14} Oxides possessing the K_2NiF_4 structure have been extensively investigated since the observation of high-temperature superconductivity in $\text{La}_{2-x}\text{Ba}_x\text{CuO}_4$ by Bednorz and Müller.¹⁵ La_2NiO_4 exhibits various structural polymorphs that are dependent on temperature and subtle changes in stoichiometry; the effect of the cooperative tilting of the NiO_6 octahedra has also been previously studied.^{6,11,16–19} Skinner¹¹ determined with the use of *in situ* high temperature neutron powder diffraction that La_2NiO_4 exhibits the tetragonal symmetry (space group $I4/mmm$) above 423 K and up to at least 1073 K. At room temperature La_2NiO_4 exhibits the orthorhombic symmetry (space group $Cmca$).²⁰

Atomistic simulation techniques provide detailed information concerning the diffusion mechanisms of materials.^{21–25} The aim

of the present study is to predict the oxygen diffusion mechanism and activation energy of migration in tetragonal $\text{La}_2\text{NiO}_{4+\delta}$ using molecular dynamics (MD). The results are discussed in view of recent experimental evidence.

Methods

MD simulations are the iterative solution of Newton's equations of motion for an ensemble of particles that interact through potential energy functions. The classical Born-like description of the ionic crystal lattice is used.²⁶ The interactions between ions i and j are described by a long-range Coulombic (summed using Ewald's method²⁷) and a short-range parameterized Buckingham pair potential.²⁸ The Buckingham pair potential is summed to the cut-off value of 10.5 Å, beyond which the influence of the potential is considered negligible. The lattice energy is given by,

$$E_L = \sum_{j>i} \sum \left[\frac{q_i q_j}{4\pi\epsilon_0 r_{ij}} + A_{ij} \exp\left(\frac{-r_{ij}}{\rho_{ij}}\right) - \left(\frac{C_{ij}}{r_{ij}^6}\right) \right] \quad (1)$$

where r_{ij} is the interionic separation, q_i is the charge of ion i , A_{ij} , ρ_{ij} and C_{ij} are the short-range parameters of the Buckingham pair potential (see Table 1) and ϵ_0 is the permittivity of free space. The short-range parameters used here were reported in previous studies,^{3,29} and their efficacy has been established for La_2NiO_4 (see ref. 3 and 7) and other oxide materials.^{30–32}

The present simulations are based on the high temperature tetragonal structure of $\text{La}_2\text{NiO}_{4+\delta}$ determined by Skinner.¹¹ The periodic crystal lattice is constructed from a supercell of $10 \times 10 \times 4$ unit cells (containing 5600 ions) tessellated throughout space through the use of periodic boundary conditions as defined by the crystallographic lattice vectors. Thermogravimetric analysis of $\text{La}_2\text{NiO}_{4+\delta}$ (ref. 33–35) has revealed a number of oxygen hyperstoichiometries that were dependent upon the thermal

Table 1 Buckingham interionic potential parameters (see eqn (1))

Interaction	A_{ij}/eV	$\rho_{ij}/\text{\AA}$	$C_{ij}/\text{eV \AA}^6$	Reference
$\text{O}^{2-}-\text{O}^{2-}$	9547.96	0.2072	32.00	29
$\text{La}^{3+}-\text{O}^{2-}$	2119.79	0.3459	23.25	3
$\text{Ni}^{2+}-\text{O}^{2-}$	905.40	0.3145	0.00	3

Department of Materials, Imperial College London, London, SW7 2AZ, United Kingdom. E-mail: alexander.chroneos@imperial.ac.uk

history of the samples and other experimental conditions. In the present study, to predict the effect of oxygen content on oxygen transport, a number of oxygen hyperstoichiometries, $0 \leq \delta \leq 0.12$, were considered. The range of δ and oxygen interstitial sites are supported by neutron diffraction studies on single crystals of $\text{La}_2\text{NiO}_{4+\delta}$.¹¹

The velocity Verlet algorithm was applied to integrate Newton's equations of motion.³⁶ Initially, ions were assigned a Gaussian distribution of velocities and with iterative velocity scaling, a stable temperature was obtained. The production runs that were used in the analysis were monitored after the system was equilibrated for 5000 time steps (~ 5 ps). The variable time step option as incorporated in the DLPOLY code was used for efficient sampling of the dynamic behavior.^{37,38} Up to 250 000 time steps (each time step of the order of 1 fs) were used to investigate oxygen diffusion in the temperature range 800–1100 K. A constant pressure (NPT) ensemble was applied to predict the equilibrium lattice parameters and a constant volume (NVT) ensemble to predict the diffusion properties with the volume of the cell set to the equilibrium value for the given temperature. We have introduced the interstitial oxygen atoms at random sites within the cell. The equilibration period of 5000 time steps in the NPT ensemble and 5000 times steps in the NVT ensemble (total equilibration period of about ~ 10 ps) is sufficient for the ions to reach quasi-equilibrium distributions. Corrections to the temperature, and the pressure were achieved using the Nosé-Hoover thermostat.^{39,40} The data were analyzed using the visual molecular dynamics package.⁴¹

Results and discussion

Anion Frenkel disorder is the dominant intrinsic disorder mechanism in both tetragonal and orthorhombic La_2NiO_4 .^{3,7} In particular, equatorial oxygen (4c) Frenkel disorder is more favorable compared to apical oxygen (4e) Frenkel disorder mechanism. This in turn implies that equatorial oxygen vacancies will be more readily available (compared to apical vacancies) and will effectively be more significant in vacancy-mediated oxygen diffusion.

La_2NiO_4 is formed from alternating NiO_2 and $(\text{LaO})_2$ layers.⁴² NiO_2 and $(\text{LaO})_2$ have different ideal translations that have to be adjusted to form a crystal with a uniform lattice spacing. To relax the stressed $(\text{LaO})_2$ layers the structure favours the introduction of intrinsic defects such as oxygen interstitials.⁴² Neutron diffraction studies determined that excess oxygen in $\text{La}_2\text{NiO}_{4+\delta}$ is accommodated as oxygen interstitials in the $(\text{LaO})_2$ layers.^{43,44} Furthermore, oxygen excess as described by δ in $\text{La}_2\text{NiO}_{4+\delta}$ leads to greater oxygen diffusion.⁵ The incorporation of oxygen interstitials and their migration in $\text{La}_2\text{NiO}_{4+\delta}$ was studied previously in detail using static atomistic simulation techniques.^{3,7,45} Interestingly, Read *et al.*⁴⁵ predicted that the oxidation reaction in La_2NiO_4 is exothermic. Frayret *et al.*,⁶ using density functional theory in conjunction with Bader's atoms in molecules theory,⁴⁶ predicted that the interstitial oxygen in $\text{La}_2\text{NiO}_{4+\delta}$ is doubly negatively charged (O^{2-}). In the present work we consider only O^{2-} ions that we initially distribute randomly.

Ionic transport was determined by monitoring the mean square displacement (MSD) of ions, as a function of time, for

a range of defect temperatures. To ensure adequate statistical sampling extensive simulation times of 300 ps were used. The MSD of an ion i at a position $r_i(t)$ at time t with respect to its initial position $r_i(0)$ is defined by

$$\langle r_i^2(t) \rangle = \frac{1}{N} \sum_{i=1}^N [r_i(t) - r_i(0)]^2 \quad (2)$$

where N is the total number of ions in the system. During the simulations lanthanum and nickel cations oscillate around their equilibrium positions. Conversely, especially at higher temperatures, oxygen ions demonstrate an increasing MSD with time. Therefore, oxygen self-diffusion is far more significant compared to cation self-diffusion on the time scales considered. Although there is no available experimental data on cation migration of $\text{La}_2\text{NiO}_{4+\delta}$, previous studies in perovskite-type oxides have determined that cation diffusion coefficients are orders of magnitude lower than oxygen diffusion coefficients.⁴⁷

The oxygen diffusion coefficient, D , is calculated from the slopes of MSD for a range of temperatures (here 800–1100 K) using⁴⁸

$$\langle [r_i(t) - r_i(0)]^2 \rangle = 6Dt + B \quad (3)$$

where $|r_i(t) - r_i(0)|$ is the displacement of an oxygen ion from its initial position and B is an atomic displacement parameter attributed to thermal vibrations.

Fig. 1 is an Arrhenius plot comparing the predicted diffusivities for, $\delta = 0.055$ and 0.12 , with previous experimental results.^{2,5,34} The latter δ value is closer to the experimentally determined values at high temperatures.^{33–35} The predicted values are in excellent agreement with the experimental data. Fig. 1 predicts an activation energy of migration is 0.51 eV, whereas previous experimental activation energies are: 0.85 eV for the dense ceramic² and 0.88 eV for the single crystal.⁵ Notably, however, recent experimental work of Sayers *et al.*³³ has revealed an activation energy for oxygen diffusion of 0.54 eV (see Table 2). The diffusivities of Sayers *et al.*³³ are in the same order of magnitude as the predicted and experimental diffusivities^{2,5,34} of Fig. 1. Interestingly, in tetragonal $\text{La}_{1.85}\text{Sr}_{0.15}\text{CuO}_{4-\delta}$ Savvin *et al.*⁴⁹ predicted, using MD, oxygen diffusivities that were higher by several orders of magnitude compared to the tracer study of Routbort *et al.*⁵⁰ on dense polycrystalline samples. Nevertheless, for $\text{La}_{1.85}\text{Sr}_{0.15}\text{CuO}_{4-\delta}$ their predicted activation energy of diffusion, 0.86 eV,⁴⁹ is in excellent agreement with the determined value of 0.84 eV.⁵⁰

Table 2 Activation energies of oxygen self-diffusion in $\text{La}_2\text{NiO}_{4+\delta}$

Methodology	E_a /eV	Comment	Reference
Experimental	0.19	Epitaxial thin film	13
Experimental	0.54	Polycrystal, TOF-SIMS	33
Experimental	0.88	Single crystal, <i>a-b</i> plane	5
Density functional theory	1.2	Interstitial mechanism	6
Static atomistic simulation	0.55 ^a	Vacancy mechanism	7
Molecular dynamics	0.51	Interstitialcy mechanism	Present study

^a Activation energy of migration.

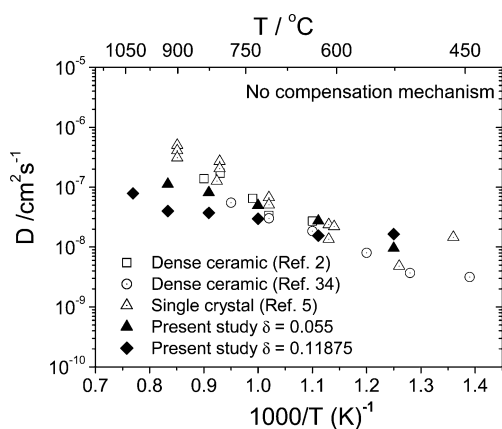


Fig. 1 Arrhenius plot of the calculated oxygen diffusivity in the a - b plane of $\text{La}_2\text{NiO}_{4+\delta}$ (for $\delta = 0.055$ or 0.11875) with no charge compensation mechanism being applied. The present results are compared with the experimental results of Skinner and Kilner,² Kilner and Shaw,³⁴ and Bassat *et al.*⁵

In the recent work by Cleave *et al.*,⁷ who considered stoichiometric tetragonal La_2NiO_4 , a number of vacancy migration pathways along the a - b plane and the c -axis were considered as well as an O^{2-} interstitial migration mechanism. These predictions indicate that the most energetically favorable mechanism for oxygen migration is the vacancy mechanism in the a - b plane.⁷ In this mechanism the oxygen vacancy is transported between equatorial sites and the overall migration activation energy is 0.55 eV.⁷ This mechanism is supported by previous simulations in the related tetragonal $\text{La}_2\text{CuO}_{4+\delta}$.^{49,51} Using static atomistic simulation techniques Cleave *et al.*⁷ considered the interstitial migration mechanism of the O^{2-} ion to be 0.86 eV. This value is in excellent agreement with the activation energy of migration for O^{2-} predicted by Minervini *et al.*³ using the same atomistic simulation technique in orthorhombic $\text{La}_2\text{NiO}_{4+\delta}$. Frayret *et al.*⁶ predicted, using DFT, a migration energy barrier *via* the oxygen interstitial mechanism of 1.2 eV. However, in addition to the

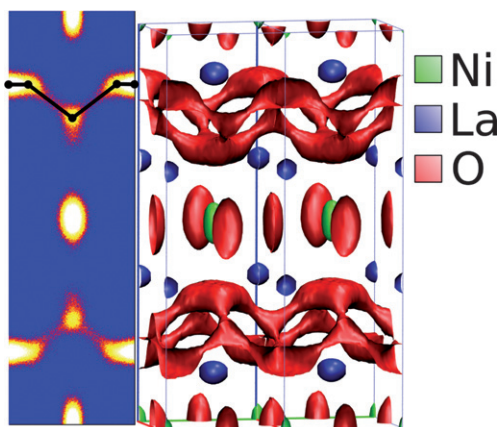


Fig. 2 Oxygen ion density in the (010) plane (left) and the isosurface connecting the oxygen conduction sites (right) from a simulation at 900 K and a delta value of 0.09 . Highlighted on the left is the proposed interstitial conduction mechanism. Also note the highly anisotropic liberation of the equatorial oxygen ions along the c -axis in agreement with the neutron diffraction data of Skinner.¹¹

small cell used in their study Frayret *et al.*⁶ only considered a direct path between the two interstitial sites, whereas in Fig. 2 we note a significant deviation from the most direct route between the lattice and interstitial site.

At this juncture it is also important to consider that vacancy mediated diffusion necessitates the formation of oxygen vacancies. Therefore, as oxygen interstitials will dominate in $\text{La}_2\text{NiO}_{4+\delta}$ over the temperature range considered, these additional oxygen ions will be accommodated in interstitial sites in the lattice (see ref. 3 and references therein). This supersaturation of oxygen interstitials greatly reduces the concentration of oxygen vacancies, through the oxygen Frenkel reaction

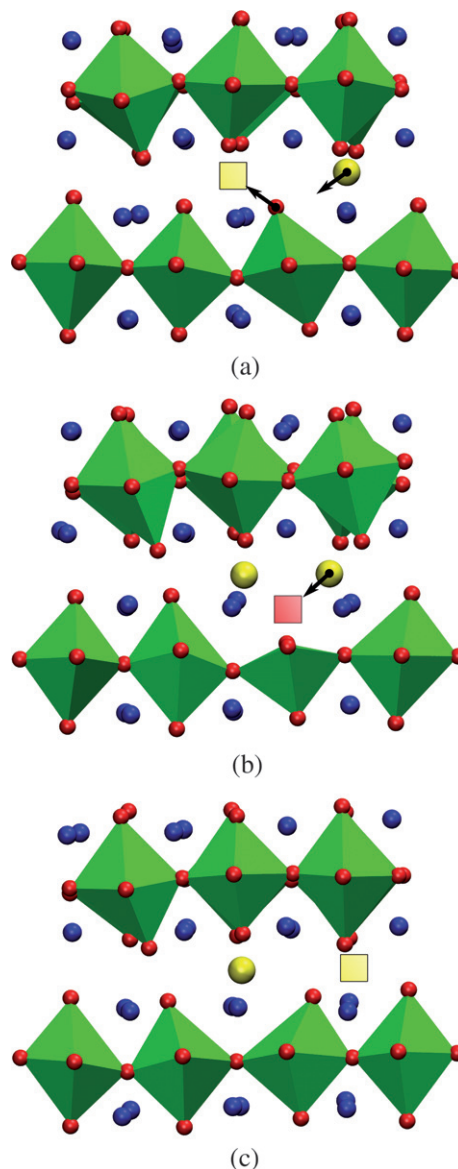


Fig. 3 (a-c): Snapshots of a typical diffusion process occurring during a molecular dynamics simulation of $\text{La}_2\text{NiO}_{4+\delta}$ at 900 K and $\delta = 0.09$. Only a small subset of ions is plotted to aid visualization. Lanthanum ions are represented by blue spheres, nickel-oxygen polyhedra are plotted in green and individual oxygen ions represented by red spheres, or yellow in the case of interstitial ions. Vacant sites relevant to the diffusion process are indicated by red and yellow squares, see text for details.

equilibrium, leading to the minimisation of diffusion by vacancy mechanisms. We also note that here, when MD simulations were carried out on perfect stoichiometric La_2NiO_4 (*i.e.* without the prior presence of either oxygen vacancies or interstitials) the oxygen diffusivities were not significant for the temperature range and time scales considered.

For a range of oxygen hyperstoichiometries, all the present predicted oxygen density profiles support an interstitialcy mechanism of diffusion in the a - b plane (see Fig. 2). In particular, the oxygen interstitial displaces an apical oxygen ion from the NiO_6 octahedron, which in turn progresses to an adjacent oxygen interstitial site. Consistent with Skinner,¹¹ we observe that the equatorial site has a strongly anisotropic thermal ellipsoid. Additionally, simulations suggest a highly anisotropic motion of the La site out of the a - b plane.

We show an example of the time resolved diffusion process in Fig. 3. Here, representative snapshots of a single simulation show ions actively involved in a single diffusion process. We note in the initial configuration (Fig. 3a) the significant tilting of the neighbouring NiO_6 octahedron away from the single interstitial oxygen ion. The apical ion from one of these octahedra is able to move upwards towards an unoccupied interstitial site with the corresponding relaxation of the existing interstitial ion towards the formerly occupied site. The intermediate state is shown in Fig. 3b and exists only briefly before the original interstitial ion reforms the NiO_6 octahedron and the apical ion takes up residence in an adjacent interstitial site. The final configuration (Fig. 3c) is equivalent to the initial configuration aside from the translation of a single interstitial ion in the a - b plane.

The intermediate state (Fig. 3b) where both ions are in interstitial sites, has a very brief residency time (~ 1 ps), however it is still possible to observe subsequent distortion of the equatorial oxygen ions towards the interstitial layer. This is the origin of the strongly anisotropic thermal ellipsoid reported from the diffraction measurements of Skinner.¹¹ It is also possible that these transient states may provide a conduction pathway for oxygen ions out of the equatorial plane. We did not observe such motion in $\text{La}_2\text{NiO}_{4+\delta}$, although other compounds with less significant anisotropy in their oxygen diffusivity may provide such a route.

Experimental evidence for oxygen interstitial transport in the a - b plane of related tetragonal materials is scarce. Notably, however, Yashima *et al.*¹⁰ recently observed an interstitial mechanism in tetragonal $(\text{Pr}_{0.9}\text{La}_{0.1})_2(\text{Ni}_{0.74}\text{Cu}_{0.21}\text{Ga}_{0.05})\text{O}_{4+\delta}$. More particularly, Yashima *et al.*¹⁰ employed neutron scattering experiments and analysis based on the maximum entropy method to demonstrate that oxygen atoms move *via* an interstitial process along a two-dimensional network in the a - b plane. Diffusion of O^{2-} ions across the a - b plane is also consistent to the MD studies of Savvin *et al.*⁴⁹ in tetragonal $\text{La}_{2-x}\text{Sr}_x\text{CuO}_{4-\delta}$.

Conclusions

In summary, MD calculations confirm the highly anisotropic nature of oxygen diffusion in tetragonal $\text{La}_2\text{NiO}_{4+\delta}$. We predict an O^{2-} interstitialcy mechanism in the a - b plane with migration activation energy of 0.51 eV. The effect of oxygen hyperstoichiometry on the activation energy is not significant. Previous theoretical evidence⁶ supports the view that charge-transfer

phenomena in $\text{La}_2\text{NiO}_{4+\delta}$ are negligible. Nevertheless, possible compensation mechanisms that could influence the oxygen transport are presently under investigation.

Acknowledgements

The authors thank Ruth Sayers of Imperial College London for useful discussions. The study was supported by UKERC from NERC TSEC program grant number: NE/C513169/1. Computing resources were provided by the HPC facility of Imperial College London.

References

- 1 V. V. Vashook, N. E. Trofimenko, H. Ullmann and L. V. Makhnach, *Solid State Ionics*, 2000, **131**, 329.
- 2 S. J. Skinner and J. A. Kilner, *Solid State Ionics*, 2000, **135**, 709.
- 3 L. Minervini, R. W. Grimes, J. A. Kilner and K. E. Sickafus, *J. Mater. Chem.*, 2000, **10**, 2349.
- 4 F. Mauvy, J. M. Bassat, E. Boehm, J. P. Manaud, P. Dordor and J. C. Grenier, *Solid State Ionics*, 2003, **158**, 17.
- 5 J. M. Bassat, P. Odierb, A. Villesuzanne, C. Marinc and M. Pouchard, *Solid State Ionics*, 2004, **167**, 341.
- 6 C. Frayret, A. Villesuzanne and M. Pouchard, *Chem. Mater.*, 2005, **17**, 6538.
- 7 A. R. Cleave, J. A. Kilner, S. J. Skinner, S. T. Murphy and R. W. Grimes, *Solid State Ionics*, 2008, **179**, 823.
- 8 H. Zhao, F. Mauvy, C. Lalanne, J. M. Bassat, S. Fourcade, J. C. Grenier and M. Pouchard, *Solid State Ionics*, 2008, **179**, 2000.
- 9 R. Sayers, J. Liu, B. Rustumji and S. J. Skinner, *Fuel Cells*, 2008, **8**, 338.
- 10 M. Yashima, M. Enoki, T. Wakita, R. Ali, Y. Matsushita, F. Izumi and T. Ishihara, *J. Am. Chem. Soc.*, 2008, **130**, 2762.
- 11 S. J. Skinner, *Solid State Sci.*, 2003, **5**, 419.
- 12 M. Schroeder and M. A. Dragan, *J. Mater. Sci.*, 2007, **42**, 1972.
- 13 M. Burriel, G. Garcia, J. Santiso, J. A. Kilner, R. J. Chater and S. J. Skinner, *J. Mater. Chem.*, 2008, **18**, 416.
- 14 G. N. Mazo and S. N. Savvin, *Solid State Ionics*, 2004, **175**, 371.
- 15 J. G. Bednorz and K. A. Müller, *Z. Phys. B: Condens. Matter*, 1986, **64**, 189.
- 16 J. D. Jorgensen, B. Dabrowski, S. Pei, D. R. Richards and D. G. Hinks, *Phys. Rev. B: Condens. Matter*, 1989, **40**, 2187.
- 17 Z. Hiroi, T. Obata, M. Takano, Y. Bando, Y. Takeda and O. Yamamoto, *Phys. Rev. B: Condens. Matter*, 1990, **41**, 11665.
- 18 J. M. Tranquada, Y. Kong, J. E. Lorenzo, D. J. Buttrey, D. E. Rice and V. Sachan, *Phys. Rev. B: Condens. Matter*, 1994, **50**, 6340.
- 19 J. M. Tranquada, J. E. Lorenzo, D. J. Buttrey and V. Sachan, *Phys. Rev. B: Condens. Matter*, 1995, **52**, 3581.
- 20 T. Kajitani, Y. Kitagaki, K. Hiraga, S. Hosoya, T. Fukuda, Y. Yamaguchi, S. Wada, S. Sugai, Y. Morii, K. Fuchizaki and S. Funahashi, *Phys. C*, 1991, **185-189**, 579.
- 21 A. Chroneos and H. Bracht, *J. Appl. Phys.*, 2008, **104**, 093714.
- 22 A. Chroneos, R. W. Grimes, B. P. Uberuaga and H. Bracht, *Phys. Rev. B: Condens. Matter Mater. Phys.*, 2008, **77**, 235208.
- 23 M. Posselt, F. Gao and H. Bracht, *Phys. Rev. B: Condens. Matter Mater. Phys.*, 2008, **78**, 035208.
- 24 A. Chroneos, H. Bracht, R. W. Grimes and B. P. Uberuaga, *Appl. Phys. Lett.*, 2008, **92**, 172103.
- 25 D. Rupasov, A. Chroneos, D. Parfitt, J. A. Kilner, R. W. Grimes, S. Ya. Istomin and E. V. Antipov, *Phys. Rev. B: Condens. Matter Mater. Phys.*, 2009, **79**, 172102.
- 26 M. Born and J. E. Mayer, *Z. Phys.*, 1932, **75**, 1.
- 27 P. P. Ewald, *Ann. Phys.*, 1921, **64**, 253.
- 28 R. A. Buckingham, *Proc. R. Soc. London, Ser. A*, 1938, **168**, 264.
- 29 R. W. Grimes, D. J. Binks and A. B. Lidiard, *Philos. Mag.*, 1995, **72**, 651.
- 30 R. W. Grimes, G. Busker, M. A. McCoy, A. Chroneos, J. A. Kilner and S. P. Chen, *Ber. Bunsen-Ges.*, 1997, **101**, 1204.
- 31 G. Busker, A. Chroneos, R. W. Grimes and I. W. Chen, *J. Am. Ceram. Soc.*, 1999, **82**, 1553.
- 32 M. R. Levy, C. R. Stanek, A. Chroneos and R. W. Grimes, *Solid State Sci.*, 2007, **9**, 588.

-
- 33 R. Sayers, R. A. De Souza, J. A. Kilner and S. J. Skinner, unpublished results.
- 34 J. A. Kilner and C. K. M. Shaw, *Solid State Ionics*, 2002, **154–155**, 523.
- 35 E. Boehm, J. M. Bassat, P. Dordor, F. Mauvy, J. C. Grenier and Ph. Stevens, *Solid State Ionics*, 2005, **176**, 2717.
- 36 W. C. Swope, H. C. Andersen, P. H. Berens and K. R. Wilson, *J. Chem. Phys.*, 1982, **76**, 637.
- 37 W. Smith and T. R. Forester, *J. Mol. Graphics*, 1996, **14**, 136.
- 38 W. Smith and I. Todorov, *The DLPOLY 3.0 User Manual*, Daresbury Laboratory, UK.
- 39 S. Nosé, *J. Chem. Phys.*, 1984, **81**, 511.
- 40 W. G. Hoover, *Phys. Rev. A: At., Mol., Opt. Phys.*, 1985, **31**, 1695.
- 41 W. Humphrey, A. Dalke and K. Schulten, *J. Mol. Graphics*, 1996, **14**, 33.
- 42 D. Brown, *The Chemical Bond in Inorganic Chemistry: The Bond Valence Model*, IUCr Monographs on Crystallography, Oxford University Press, 2002.
- 43 W. Paulus, A. Cousson, G. Dhalenne, J. Berthon, V. Revcolevschi, S. Hosoya, W. Treutmann, G. Heger and R. Le Toquin, *Solid State Sci.*, 2002, **4**, 565.
- 44 T. R. Wagner and M. O’Keeffe, *J. Solid State Chem.*, 1988, **73**, 211.
- 45 M. S. D. Read, M. S. Islam, F. King and F. E. Hancock, *J. Phys. Chem. B*, 1999, **103**, 1558.
- 46 R. F. W. Bader, *Atoms in Molecules: A Quantum Theory*, Clarendon Press, Oxford, 1990.
- 47 S. Miyoshi and M. Martin, *Phys. Chem. Chem. Phys.*, 2009, **11**, 3063.
- 48 M. J. Gillan, *Physica B*, 1985, **131**, 157.
- 49 S. N. Savvin, G. N. Mazo and A. K. Ivanov-Schitz, *Crystallogr. Rep.*, 2008, **53**, 291.
- 50 J. L. Routbort, S. J. Rothman, B. K. Flandermeyer, L. J. Nowicki and J. E. Baker, *J. Mater. Res.*, 1988, **3**, 116.
- 51 N. L. Allan and W. C. Mackrodt, *Philos. Mag.*, 1991, **64**, 1129.